Assembly of Droplet Reinjection-MS Interfaces: Overcoming Droplet Coalescence for High Throughput Screening Applications.

Emily E. Kempa,[1] Clive A. Smith,[2] Xin Li,[2] Depanjan Sarkar,[1] Denis Morsa,[3] Reynard Spiess,[1] Anouk M. Rijs [4,5] and Perdita E. Barran [1,*]

1. Michael Barber Centre for Collaborative Mass Spectrometry, Manchester Institute of Biotechnology, Manchester M1 7DN, United Kingdom.
2. Sphere Fluidics Limited, McClintock Building, Suite 7, Granta Park, Great Abington, Cambridge CB21 6GP, United Kingdom.
3. Mass Spectrometry Laboratory, UR MolSys, University of Liège, Liège 4000, Belgium.
4. Division of Bioanalytical Chemistry, Department of Chemistry and Pharmaceutical Sciences, Amsterdam Institute of Molecular and Life Sciences, Vrije Universiteit Amsterdam, De Boelelaan 1105, 1081 HV Amsterdam, the Netherlands.
5. Centre for Analytical Sciences Amsterdam, 1098 XH, Amsterdam, the Netherlands.

*** Corresponding author.**

Abstract

Droplet microfluidics coupled with mass spectrometry is evolving for high throughput screening. A commercial solution that can readily interface to existing mass spectrometry instrumentation would be highly desirable and allow the technology to become accessible to those without experience in droplet microfluidics. Here, we demonstrate a droplet reinjection workflow to infuse samples into three common mass spectrometers, each with different electrospray ionisation (ESI) source configurations. The ease of chip-mass spectrometry (MS) coupling is explored and difficulties highlighted. Particular attention has been turned to ESI sources which apply the electrospray voltage directly to the incoming droplet emitter ('push source'), as these were found to cause droplet coalescence within the microfluidic chip reinjection channel. To overcome such a difficulty, we have identified different solutions including a grounded mesh insert as a shielding approach, and minor changes to chips and ESI sources to stabilise incoming droplets. Results obtained allow the mass spectrum of individual reinjected droplets to be determined without hindrance from the electrospray voltage. The problems and solutions identified here, outline the foundations for the development of a commercial droplet reinjection-mass spectrometry interface.

Introduction

Screening technologies with the ability to analyse up to tens of thousands of samples per day are highly sought-after throughout the pharmaceutical and biotechnology sectors. [1–8] Current high throughput screening methodologies are highly reliant upon microtiter well plates. [9–13] Although, these plates are easily transferable between robotic platforms and analytical techniques,[14] their use can result in unnecessary single-use plastic and reagent waste, in addition to increased storage requirements for assays necessitating numerous plates. Droplet microfluidics provides an alternative to microtiter plates, with each droplet (pL to nL in volume) acting as a self-contained reaction vessel suspended within an immiscible liquid phase,[15–20] eliminating the need for plastic wells. Further to this, miniaturised flow devices or 'microfluidic chips' allow for the manipulation and analysis of these vessels in situ, eradicating transferal (of plates) between equipment.

Label-free analytical techniques such as Mass Spectrometry (MS), NMR, and Raman spectroscopy provide direct analytical measurements reliant on the intrinsic physical properties of a sample. [21–23] Their ability to produce sample measurements without the incorporation of florescent chromophores or radioactive isotopes is highly advantageous, as the incorporation of such labels can be expensive and requires additional method development to ensure suitability within the sample matrix. Although a number of these label-free techniques have been successfully coupled with microfluidics, [16,23–26] coupling with droplet microfluidics remains more difficult due to its dual-phase nature. Harnessing this property, however, allows for the exploitation of droplet microfluidics for high throughput screening technologies.

The approach explored here is the use of droplet-reinjection methodologies to design a high throughput MS platform for the analysis of a biotransformation within droplets. Generation of droplets containing biotransformation reagents (and possibly cellular material), followed by reinjection on to the analytical system of choice allows for chemical reactions (and/or cellular

incubation) to occur within droplets under a time frame determined by the interval between the two aforementioned steps. Manipulation of such a time frame can allow reaction kinetics occurring within the droplets to be realised. [27–29] Bio-reactions relying upon the encapsulation of genetic variations within droplets, is also applicable to this approach, as organisms such as bacteria, [30] yeast [31] and fungi [32] have all been shown to proliferate within droplet systems. An example of this is given in Figure 1, indicating the growth of *E. coli* bacterial colonies within 450 pL droplets. Subsequent reinjection of such a droplet population onto a suitable analytical system would allow for heterogeneity between colonies to be identified.

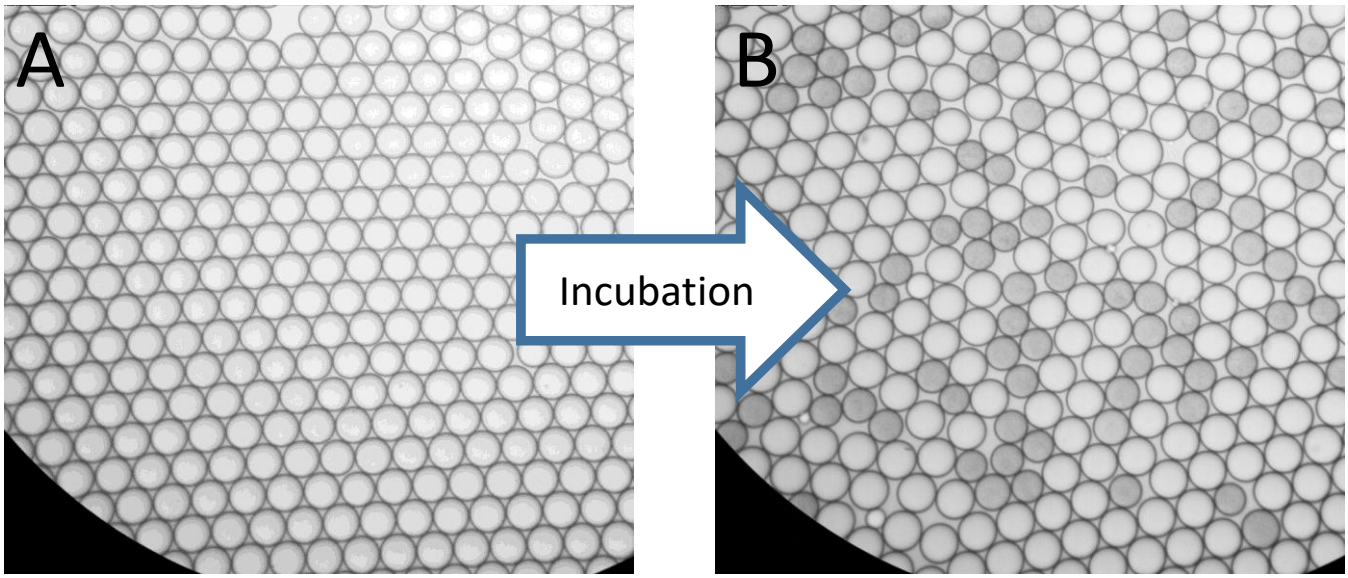

Figure 1A) Phase contrast microscope image of highly monodisperse droplets (~450 pL) containing bacterial cells before incubation. B) Phase contrast microscope image of the droplet population after incubation (overnight, 30 °C). Grey droplets indicate the growth of a bacterial colony inside the droplet. White droplets indicate a cell-free (empty) droplet, i.e., no encapsulated bacteria to proliferate into a colony during incubation.

Droplet reinjection-MS has been demonstrated in the literature by several academic groups, [33–38] each utilising a unique microfluidic–mass spectrometry setup. Smith *et al*. demonstrated in 2013 the reinjection of protein-filled droplets, with the protein contents of each droplet

identifiable via the MS data. [36] Belders' group have furthered this in several publications in which they have reinjected droplets containing different types of actinobacteria, incubated both on [39] and off-chip. [37,40] They have also demonstrated the ability to generate droplets, incubate bacteria, perform a biocatalytic reaction, reinject droplets and couple with MS, all within one device. This device allowed for reaction monitoring of amino acid production inside the droplets over 8 hours. [39] Although this group has successfully demonstrated an application of droplet reinjection, to date, this has involved the complete redesign of electrospray ionisation (ESI) sources. An equivalent commercial solution coupling droplet microfluidics with MS is yet to become widely available, with only one notable platform, the ESI-Mine™ (Sphere Fluidics Ltd, Cambridge, UK) [41] available on the market. This platform is built upon a Perkin Elmer AxIon II mass spectrometer which has recently been discontinued. Here we explore the reinjection workflow and the hardware implications of such a platform. In particular, we focus upon utilising ESI apparatus most commonly supplied with the purchase of popular (nano)-liquid chromatography (LC)-MS systems.

Reinjection Workflow

A droplet reinjection-MS experiment in its simplest form consists of 4 steps: droplet generation, droplet storage, reinjection into the MS, and data visualisation (Figure 2A). Initially, droplets of the required size (500 pL - 1000 pL) and contents are generated using a microfluidic chip with flow focusing, T-junction, or coaxial geometry, [42] before being collected in a suitable vessel (step 1). Subsequently, the droplets are stored (and/or incubated) until the desired analysis time (step 2). The reinjection of droplets can then occur within a microfluidic chip containing a 'Y-shaped' channel configuration. Use of the infusion flow rates determines the length of separation between droplets within the flow channel (assuming plug-like flow is occurring within the channels). These droplets are then introduced into the MS one at a time in rapid succession, via an ESI needle

emitter incorporated into the reinjection microfluidic chip (step 3). [36] Primary data output consists of a total ion chromatogram (TIC) in which each observed peak consists of one droplet reaching the MS detector. Akin to chromatography, the mass spectrum for each peak can be obtained, thus indicating individual droplet contents (step 4).

Although coupling droplet microfluidics with MS has been described previously by many groups, differences between ESI source types were not explicitly compared until work by Peretzki *et al*. in 2020. [43] In this body of work we have divided the two major ESI source types into those which apply the electrospray voltage directly to the incoming capillary emitter or solution ('push' type, Figure 2B), and those which maintain the incoming capillary emitter at ground potential with respect to the MS inlet voltage ('pull' type, Figure 2C). Although both types have their advantages and work equally well for LC-MS or direct infusion experiments, their applicability to a droplet microfluidic interface is more complicated due to the dual-phase nature (water-in-oil) of the incoming droplet emulsion. The most notable difficulty is the effect of the 'push' source electrospray voltage located directly on the incoming droplet solution. Although the application of electrical voltages to solutions is a well-exploited approach within digital microfluidics to move and divide droplets, [44] in this case, the electrical potential results in the unwanted disruption of the droplet form. [43] Examples of this phenomenon and viable solutions to control unwanted droplet disruption for reinjection experiments are explored later in this article.

Methods and Materials

Ammonium acetate was purchased alongside leucine enkephalin, phenylalanine (F) and diphenylalanine (FF) from Sigma-Aldrich (Dorset, UK). Leucine enkephalin was dissolved in a solution of 100 mM ammonium acetate in deionized water (Milli-Q Advantage ultrapure water filtration system, Merck Millipore, Darmstadt, Germany) to produce a ~20 µM solution.

Phenylalanine (F) and diphenylalanine (FF) were dissolved in water to produce solutions of 100 µM and 280 µM respectively.

Chip Design and Fabrication

All microfluidic chips used in this work were fabricated from polydimethylsiloxane (PDMS, SYLGARD™ 184 Silicone Elastomer Kit, Dow Chemical Co., MI, USA) using established photolithography and soft lithography techniques as described in the literature. [45,46] Chip designs utilised can be found in the supporting information to this article (Figure S1). Two differing types of integrated ESI emitters were used in the experiments. Primarily, stainless steel capillaries (OD: 176 µm, ID: 76 µm, various lengths as stated), (Vita Needle Co., Needham, MA, USA,) were utilised with pull source instrumentation (Figure 4), and the initial push source interface (Figure 6A & B). Fused silica capillaries (OD 150 µm, ID 75 µm, Polymicro Technologies, LLC, Phoenix, AZ, USA) were subsequently used as the emitter type for push source solutions (Figure 9). These fused silica capillary pieces were cut to 6 cm in length and their outer surfaces sputter coated in aluminium before insertion into the final microfluidic device. Both emitter types were incorporated into the fluidic outlet channel of the final PDMS devices and secured using ELASTOSIL E43 silicon sealant (Wacker Chemie AG, München, Germany) as described by Wink *et al*. [37] Copper gauze (60 mesh woven from 0.19 mm diameter wire, Alfa Aesar, Haverhill, MA, USA) utilised as a push source solution was also incorporated into some PDMS devices as stated. A detailed procedure for emitter and copper gauze insertion can be found in the Supporting Information.

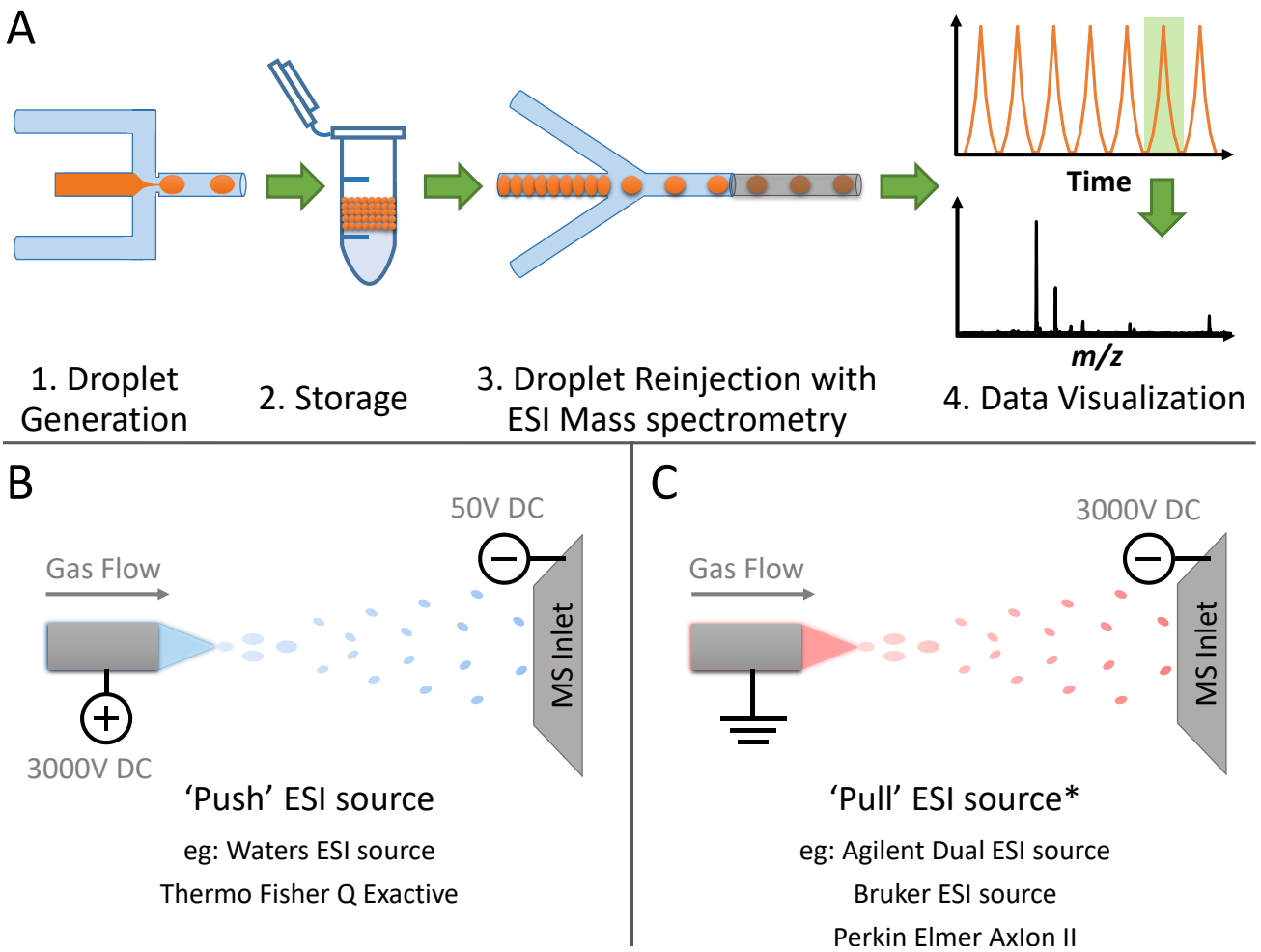

Figure 2: A) Workflow indicating the major steps and results expected in a typical droplet-ESI-MS experiment. Initially, droplets are generated using a microfluidic chip, before storage (and/or incubation) of the droplets in a suitable vessel. After storage, droplets are 'reinjected' into the mass spectrometer via a 'Y-shape' configuration microfluidic chip containing an ESI needle outlet. Typical chromatographic results are shown in which each peak in the chromatogram represents an individual droplet. Mass spectra from each droplet can be obtained. B) Example schematic representation of a 'push' ESI source, in which a voltage is applied to the incoming sample solution before the MS inlet. C) Example schematic representation of a 'pull' ESI source, in which the incoming sample solution is held at ground potential before the MS inlet.

Droplet Generation, Storage and Reinjection

Droplet generation was achieved using a Picodroplet Single Cell Encapsulation System (Sphere Fluidics Ltd, Cambridge, UK) in which the separative oil phase consisted of Pico-Surf™ 1 (Sphere Fluidics Ltd, Cambridge, UK) diluted to 1% in Novec™ 7500 Engineered Fluid (3M, Maplewood, MN, USA). Droplet collection occurred within a reinjection syringe initially filled with Novec™ 7500 Engineered Fluid as described in Figure 3 (steps 1-3) and allowed for the facile transfer between encapsulation system and mass spectrometer. When not in use, droplet containing reinjection syringes were stored at +4°C (Figure 3, step 4).

Droplet reinjection was achieved via connection of the reinjection syringe outlet (Figure 3, step 5) and spacing oil reservoir to the microfluidic chip using 1.09 mm OD tubing (0.38 mm i.d., Smiths Medical Inc., Minneapolis, MI, USA). Infusion flow rates were controlled using a neMESYS low-pressure syringe pump (CETONI GmbH, Korbußen, Germany) in each case. Droplet infusion was achieved via the flow of Novec™ 7500 Engineered Fluid to the base of the reinjection syringe, in which the upward flow of the oil phase displaced the droplet population, subsequently pushing them toward the chip spacing region (Figure 3, step 5). Reinjection spacing oil consisted of Novec™

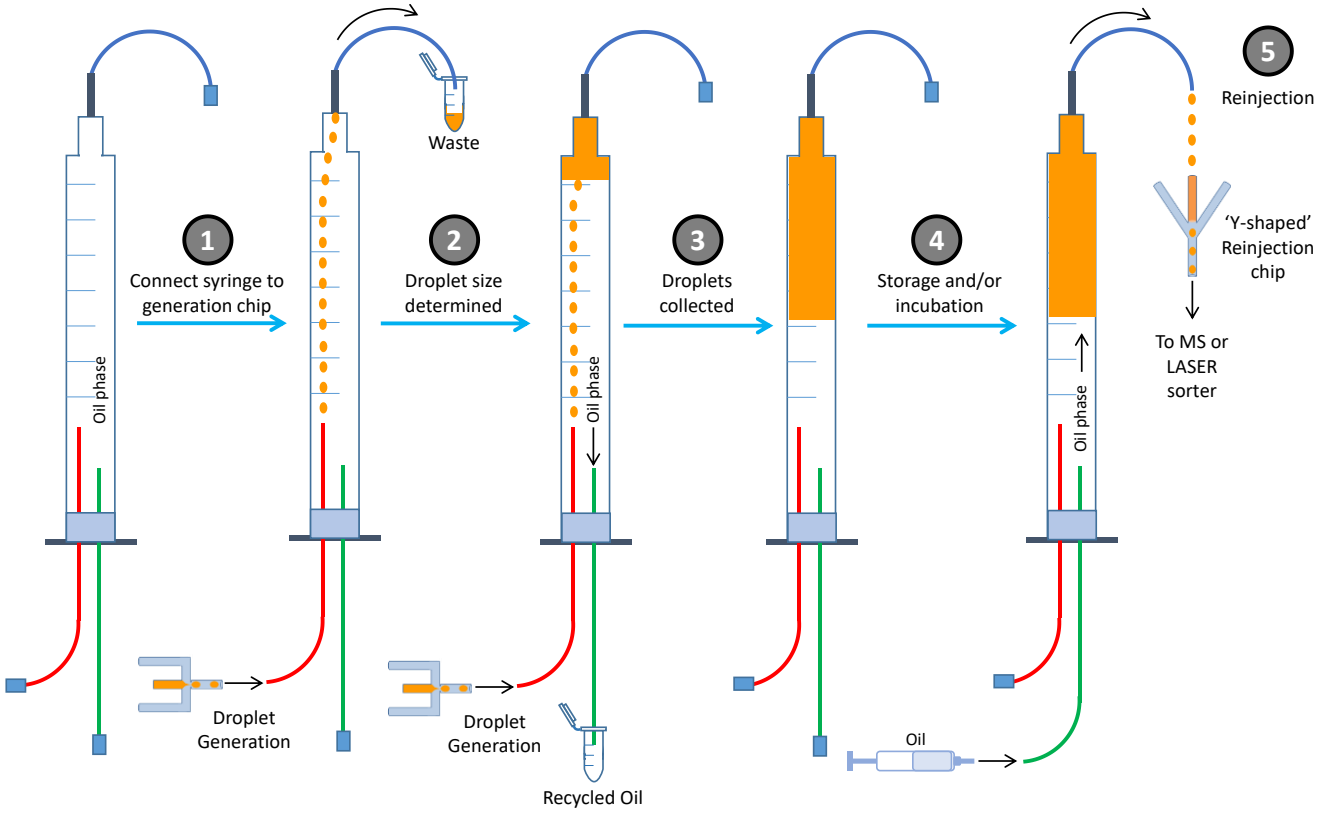

Figure 3: Schematic indicating the major stages of generating, collecting, storing, and reinjecting droplets using a reinjection syringe. 1. Reinjection syringe filled with the chosen oil phase. 2. Syringe inlet connected to the generation chip outlet and droplets allowed to flow up and out of the syringe into waste. 3. Upper outlet capped and lower outlet opened to let oil drain away as incoming droplets rise to the top and are trapped in the syringe. 4. All inlets and outlets capped and syringe containing droplets stored and/or incubated. 5. Syringe inlet connected to spacing oil and droplets pushed out the top of the reinjection syringe and through the 'Y shaped' reinjection chip into the MS.

Pull Source Assembly and Results

Coupling of the droplet reinjection-microfluidic chip with a pull source was achieved on two MS vendors' instrumentation, both utilising ESI sources with considerably similar designs. Both required the incorporation of a stainless-steel emitter of approximately 12 cm in length into the microfluidic chip. Coupling to a 6560 IM-Q-TOF (Agilent Technologies, Santa Clara, CA, USA) with a Dual-ESI source is as described in Figure 4. The assembly is based largely upon the standard Dual-ESI setup, but with the ESI-needle supplied by Agilent removed. This removal allows for the steel emitter of the microfluidic chip to be passed through the entirety of the nebuliser block until the emitter protrudes from the original needle outlet. The level of protrusion can be altered via movement of the microfluidic chip glass slide along the vertical axis, prior to the supporting glass slide being clamped in place. The fluidic connections can then be carefully added to the microfluidic chip. As described in Figure 4B, the entirety of the nebuliser block is held at ground potential, in a perpendicular arrangement to the MS inlet. A comparable assembly was also achieved with an amaZon SL dual funnel electrospray ionization quadrupole ion trap (ESI-QIT) mass spectrometer (Bruker Daltonics Inc., Billerica, MA, USA) with the schematic for this given in Figure S4A.

Infusion of ~600 pL droplets containing leucine enkephalin (20 µM solution) via the chip-pull source arrangement in Figure 4 yielded the expected chromatographic results (Figure 5A). The peaks visualised in the chromatogram each represent one droplet detected by the mass spectrometer, with the spaces between peaks indicating the time between droplets in which the oil is exiting the chip emitter. Note that the oil phase does not ionise readily in positive ionisation mode, and thus is not detected by the mass spectrometer in this mode. Subsequently, the mass spectrum of each droplet can be visualised via the extraction and summation of the MS data under the selected peak as shown in Figure 5B, with the protonated species of leucine enkephalin $[M+H]^+$

observed at *m/z* 556.3. The frequency of droplet reinjection can also be determined via the chromatogram, and in this case, droplet detection is observed at ~8 droplets/s. Alteration of this frequency (for this droplet volume and others) can be accomplished by changing the flow rates in the droplet infusion and spacing oil channels. Upon increasing the droplet volume (and thus diameter), the droplet reinjection frequency will decrease (when infused under identical flow rates). Data supporting the reinjection of alternative droplet sizes (600 pL, 765 pL and 1075 pL) via this apparatus can be found in Figure S14.

Data exhibiting the infusion of droplets (1.25 nL) into the analogous ESI-QIT set up can be found in supporting information Figures S12 and S13. This data supports the pull source apparatus assembly for both droplet generation-MS (as in Kempa *et al*. [47]) and droplet reinjection-MS. [48]

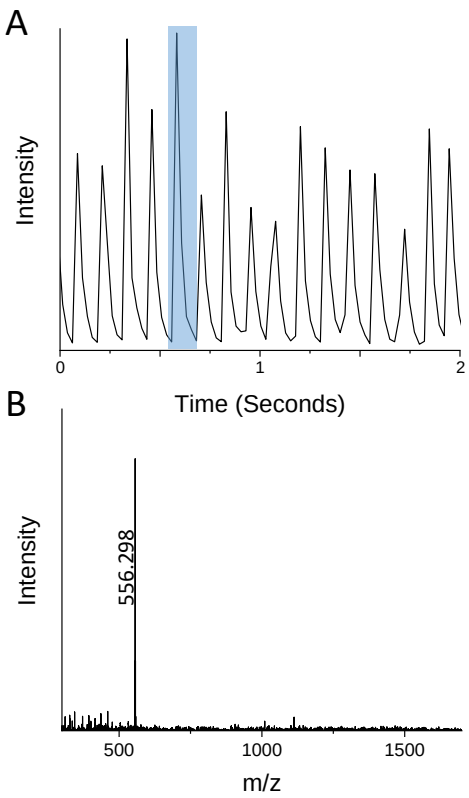

Figure 4: A) Total ion current (TIC) chromatogram obtained from reinjection of ~600 pL droplets via the chip-Agilent-ESI interface into an Agilent 6560 Mass Spectrometer. Each peak indicates detection of an individual droplet, with an approximate infusion frequency of 8 droplets/s. MS scan rate is 40 spectra/s B) Mass spectrum obtained from 1 droplet peak (summation of two scans as indicated in the blue shaded rectangle). The droplet contains 20 µM of Leucine enkephalin peptide, [M+H]+ = 556.298 m/z

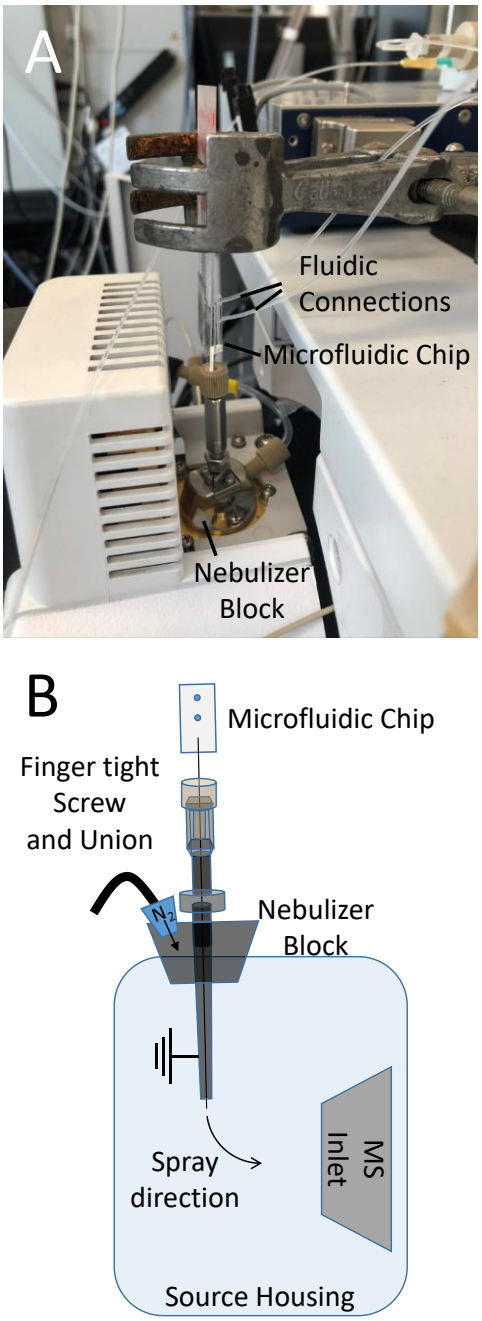

Figure 5: A) Photograph of a microfluidic chip containing a stainless-steel emitter outlet interfaced with an Agilent Dual-ESI source. The emitter outlet has been threaded through the beige finger tight screw and the nebuliser block. The glass slide containing the PDMS microfluidic chip is held in place with a clamp stand. B) Schematic representation (cross-section view) of the chip-Agilent-ESI interface indicating the emitter position threaded through the nebuliser block and held at ground potential wrt to the MS inlet.

Push Source Assembly and Results

Chip coupling to a push source (Synapt G2-Si Q-TOF, Waters Corp., Milford, MA, USA) is as described in our previous publication [47] with a schematic and photograph of this interface given in Figure 6A and B. Briefly, the microfluidic chip with 6 cm stainless-steel emitter is threaded

through the sprayer component of a Waters NanoLockSpray ESI source in the place of a picotip emitter or nanospray column. Voltage is applied to the entirety of the sprayer assembly to induce an electrospray from the emitter outlet, which is then directed into the MS inlet (cone) via a voltage gradient and the MS vacuum. As with the pull source arrangement, fluidic inlets can be connected to the microfluidic chip to begin the droplet reinjection experiment. After numerous attempts, and experimentation with differing MS source parameters, it was clear that a steady droplet reinjection trace could not be achieved using this assembly. An example of this is given in Figure 6C, in which peaks that should correspond to stable droplet reinjection are instead differing widely in arrival frequency and peak intensity.

A secondary observation was made inside the tubing leading from the reinjection syringe to the microfluidic chip. Upon initial connection, the droplet emulsion appeared uniform throughout the length of the tubing, however, a short time after application of the electrospray voltage, this uniformity diminished and instead was replaced with interspersed bands of oil and aqueous phase. This observation indicated that the electrical field generated by the applied voltage in the proximity of the microfluidic chip and reinjection syringe was disrupting the droplet population. This confirms the total ion chromatogram obtained in Figure 6C results from disrupted and coalesced droplets entering the mass spectrometer, and thus, in this configuration, the push source is not suited to droplet reinjection.

To further understand and visualise the effect of the voltage upon droplets residing in the chip, the chip, threaded through the sprayer head, was interfaced with the Picodroplet Single Cell Encapsulation System. Using an external HV amplifier (Advance Energy PLC, UK) a +1 kV voltage was placed on the sprayer head, thus applying a voltage to the chip emitter. Images obtained from the microscope high-speed camera (Mikotron-GmbH, Unterschleißheim, Germany) indicated that

upon bringing the voltage in proximity, and onto the chip emitter, the coalescence of droplets travelling through the spacing region occurred (Figure 7). The frequency of coalescence events was irregular, and the larger droplets generated post-coalescence at the 'Y' shaped junction varied in size. The mechanisms for this phenomenon are explored in more detail in the extended discussion. These coalescence events and consequent mixing of droplet contents confirmed that the droplets initially generated and stored in step 1 and 2 of the reinjection workflow (Figure 2A) are no longer intact. Hence, a droplet reinjection-MS experiment in this push source arrangement is not fit for purpose.

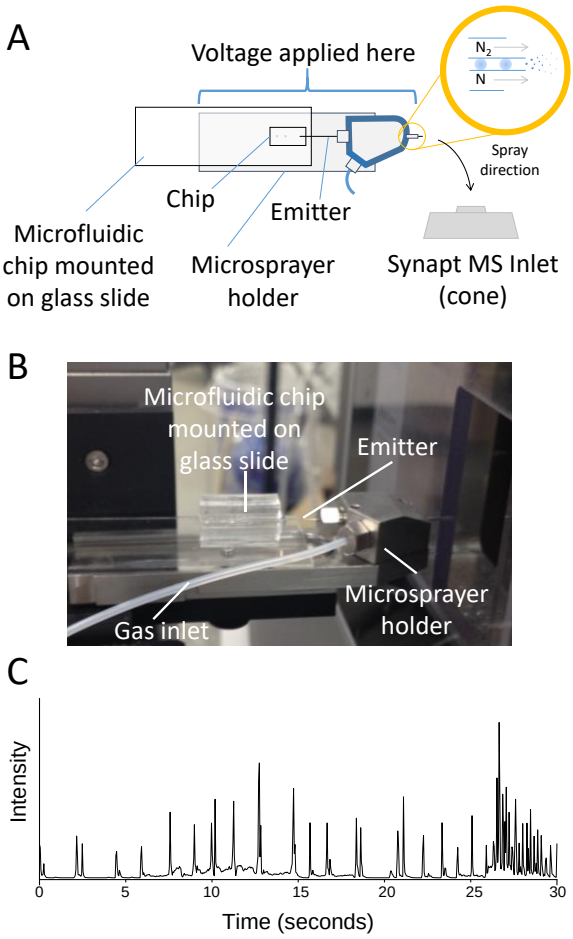

Figure 6: A) Schematic representation of a droplet microfluidic chip interfaced with a Waters sprayer, as mounted on a Waters nanoESI source. The emitter outlet of the chip has been threaded through the sprayer head to which the electrospray voltage is applied. A gas flow (N2) perpendicular to the emitter may be used to aid the electrospray (yellow ringed inset). B) Photograph of the chip-sprayer interface mounted on a Waters nanoESI source. C) TIC obtained from a droplet reinjection experiment using a Waters Synapt G2-Si mass spectrometer with nanoESI source and chip-sprayer interface. No stable droplet trace is obtained.

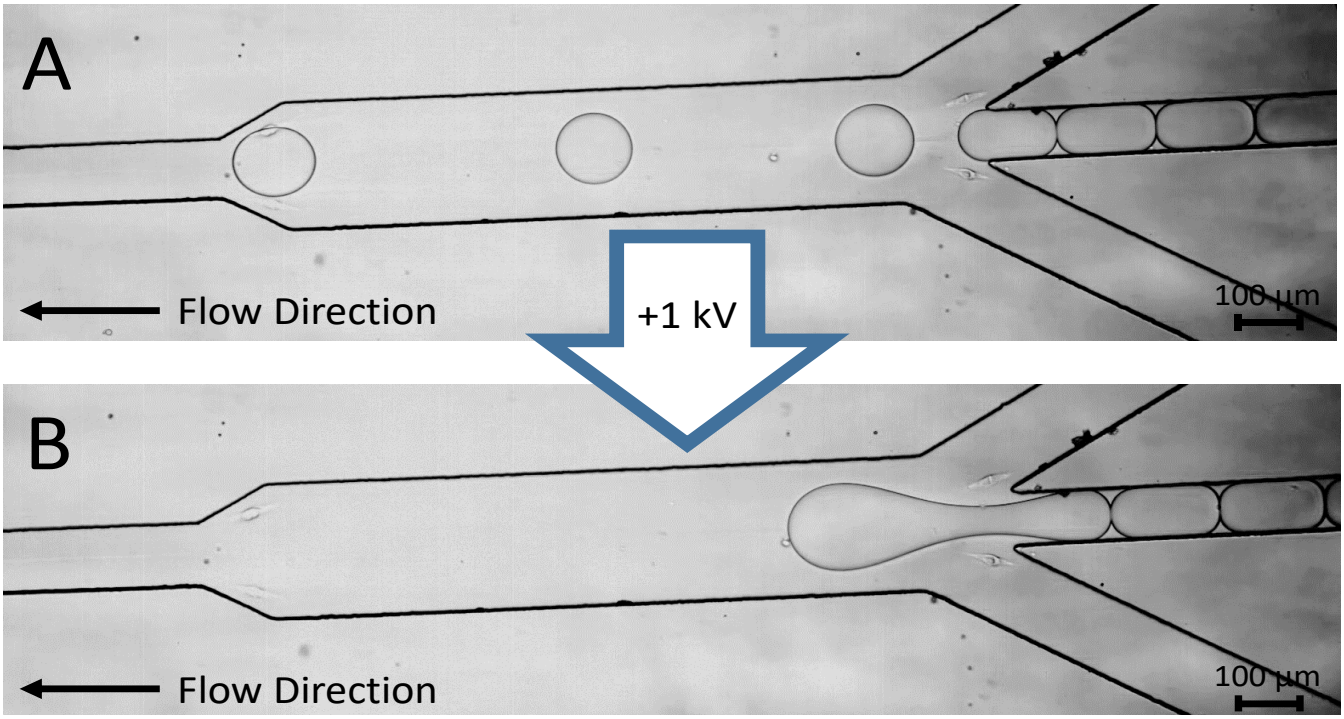

Figure 7: A) Microscope image of stable droplet reinjection using chip design 1 before application of a voltage on the conductive emitter outlet. B) Microscope image indicating coalescence of pre-generated droplets in the droplet spacing region upon application of +1 kV on the conductive emitter outlet.

Push Source Solutions

To find a push source arrangement suitable for droplet reinjection, several modifications to the setup were employed. The most notable alteration being the insertion of copper gauze into the PDMS chip (design 2, Figure S1) perpendicular to the channel plane (Figure 8A, Figure S3) akin to the method described by Schirmer *et al*. [39] The finished microfluidic device with gauze and stainless steel emitter were interfaced with the Picodroplet Single Cell Encapsulation System as in Figure 8B, with the emitter passed through the sprayer head (supported on a glass slide) as it would be on the MS. The copper gauze was connected to an external grounding plug using a crocodile clip and the fluidic connections inserted into the chip to achieve the desired reinjection flow through the droplet spacing region. The voltage from the HV amplifier was placed on the sprayer head via a probe as seen in Figure 8B. As observed in Figure 8D, the copper gauze when

connected to the grounding plug shields the reinjection region from the electric field emanating from the voltage placed on the sprayer head and emitter. When disconnected from ground potential (Figure 8C), the electric field can once again penetrate the droplet reinjection region and droplet coalescence returns.

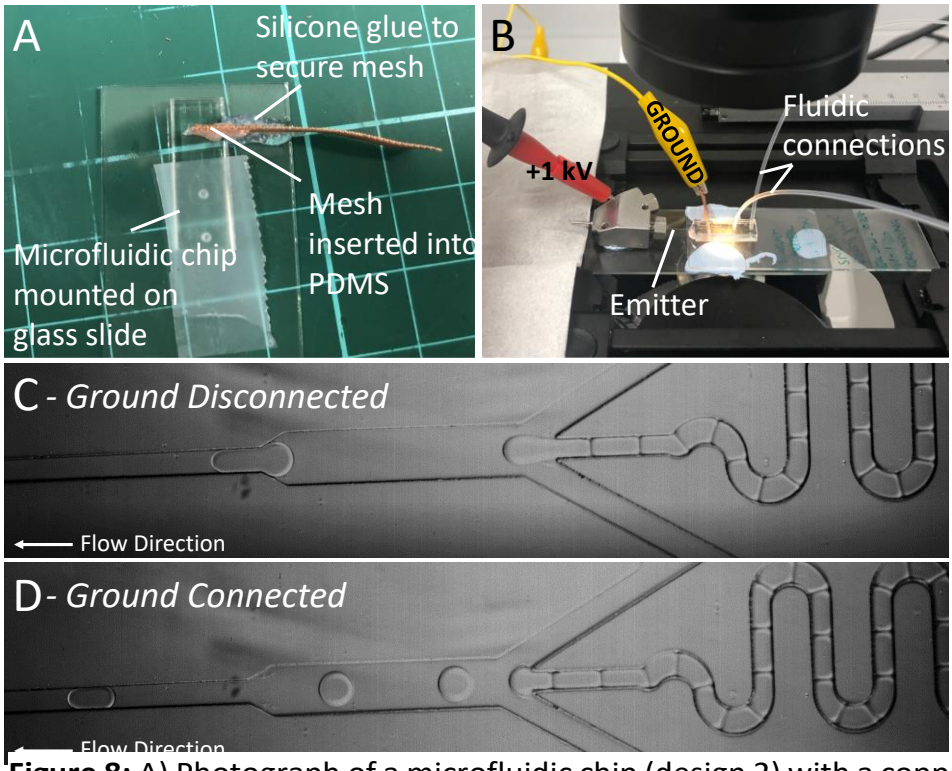

Figure 8: A) Photograph of a microfluidic chip (design 2) with a copper mesh inserted into the PDMS to shield the reinjection region from the electrospray voltage. N.B. Photograph was taken before insertion of the electrospray emitter. B) Photograph of the microscope-chip assembly used to test the shielding properties of the copper grounding mesh on droplet reinjection. The yellow crocodile clip is connected to a grounding plug and the red probe to a HV amplifier. C) Grounding clip disconnected - Microscope image of droplet coalescing in the chip spacing region upon 1 kV application on the emitter and sprayer head. D) Grounding clip connected - Microscope image of stable droplet reinjection in the chip spacing region upon 1 kV application on the emitter and sprayer head.

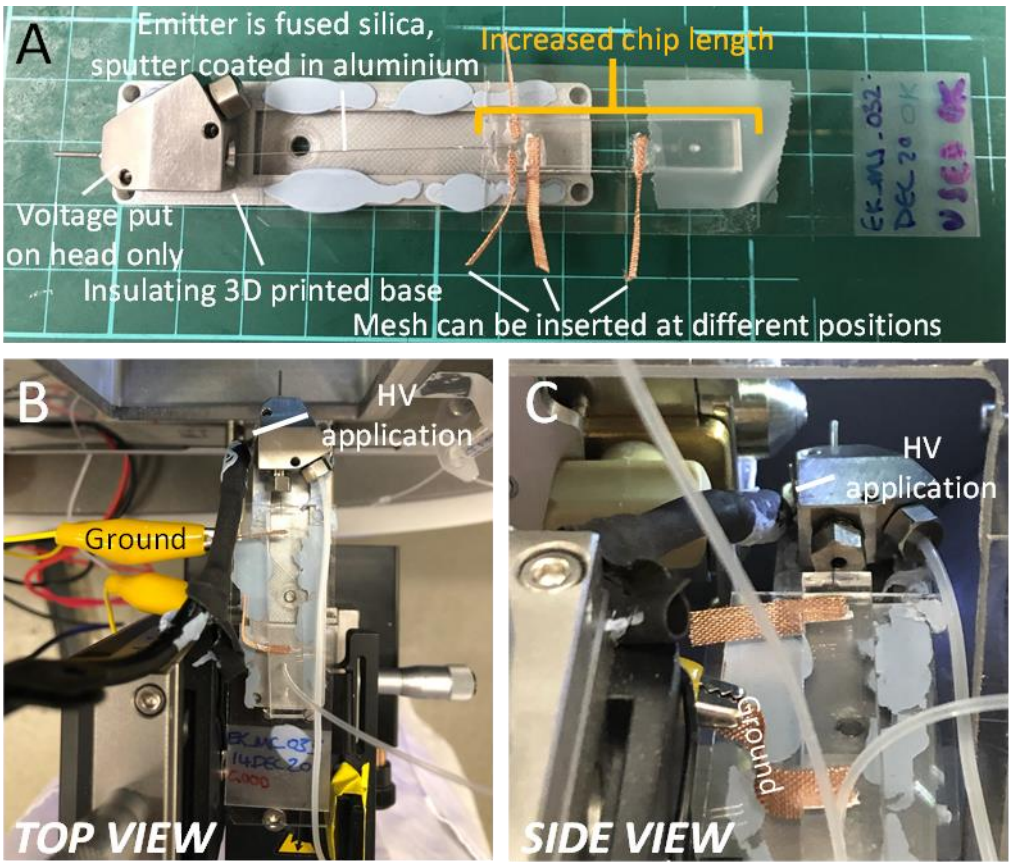

Figure 9: A) Photograph of the sprayer head fixed to a 3D-printed base (silver plastic) on which the microfluidic chip containing grounding mesh sits. The emitter outlet is threaded through the sprayer head and the chip distance from the head is adjusted until the emitter end protrudes from the sprayer head exit. B) Top view photograph of the base, chip, and sprayer head in A interfaced with a Waters NanoLockSpray source. The grounding mesh has been connected to a ground potential using the yellow crocodile clip. The ESI HV cable has been removed from the base of the stage and connected directly to the sprayer head. The stage remains at ground potential. C) Side view photograph of the base, chip, and sprayer head in A interfaced with a Waters NanoLockSpray source, indicating the position of the HV application on the sprayer head and the proximity to the MS inlet (cone).

Additional observations made from the microscope analysis found the use of stainless steel emitters to disrupt the droplet form at the chip exit (Figure S6). The direct application of voltage to the droplet via the steel emitter caused unwanted splitting and tailing of the droplet. Hence, the emitter material was changed to fused silica with an outer coating of aluminium. As the emitter inner surface was no longer electrically conductive, droplet splitting at the chip exit ceased (Figure S7). The aluminium conductive coating now served as the point of ESI voltage application.

To further negate the effects of the electric field upon the incoming droplets, and to ensure higher voltages could be placed upon the emitter, two other modifications from reinjection designs were employed. Firstly, an elongation of the chip (designs 3 and 4, Figure S1) to further distance incoming droplets from the applied voltage as described by Peretzki *et al*. [43] Secondly, alteration of the NanoLockSpray source to incorporate a 3D printed sprayer base. [49] Both of these modifications are depicted in Figure 9A.

Incorporation of the 3D printed base was necessary to insulate the microfluidic chip further from the voltage source. Utilising the standard Waters sprayer component (Figure S8A) fabricated from stainless steel carried the voltage and electric field underneath the PDMS microfluidic chip, thus causing coalescence and rendering the shielding mesh useless. This change in sprayer base material did, however, require movement of the ESI high voltage (HV) cable connection from beneath the sprayer block, too directly onto the sprayer head (Figure 9B and C). This was secured using silver conductive paint (RS Components, Corby, UK). The grounding cable to the stage remained in place and additionally served as the ground connection for the inserted copper gauze (Figure S10). Note, some removal of the outer cable heat shrink sleeve was required for the cable to stretch to its new position.

Using the modifications described above to shield droplets from the electrospray voltage, reinjection of single 1 nL leucine enkephalin (20 µM solution) droplets on a push source was

successful. This is depicted by the chromatogram obtained in Figure 10A. Regular rises and falls in the TIC indicate the detection of individual droplets as they are infused into the MS at a rate of ~3.5 droplets/s. Mass spectra of individual droplet contents can then be extracted (Figure 10B) indicating the presence of leucine enkephalin m/z. As to be expected, increasing the droplet channel flow rate results in an increased reinjection frequency (Figure 10C, ~8.5 droplets/s). The spacing oil flow rate remained constant in both cases (200 µL/hr).

Discussion

The fusion of two liquid components can be achieved within Lab-on-a-Chip (LOC) technologies using a variety of methods, including in-flow, [50,51] light-activated, [52] and electro-coalescence. [53,54] The controlled manipulation of droplets using an electric field within droplet microfluidics (and in particular digital microfluidics [44]) is well-established, allowing for the dispensing, movement, splitting, merging [55,56] and sorting of droplets. [57] The unwanted and un-controlled electro-coalescence demonstrated in Figure 7 however, posed a major stumbling block to the reinjection of droplets using the push ESI source arrangement. The cause and mechanisms surrounding this phenomenon have been elegantly described by Zagnoni *et al*. [58] One proposed cause of such 'upstream' coalescence is the effect of the electric field upon the stabilising surfactant molecules at the droplet-oil interface. In the absence of the electric field, the surfactant molecules prevent 'passive' coalescence while droplets are within the flow device. [59] The application of the penetrating electric field causes the polar surfactant molecules to re-orientate due to the electric force exerted over their dipoles. This reorientation generates variations in the surface tension along the droplet surface, with some regions becoming depleted of surfactant molecules. This

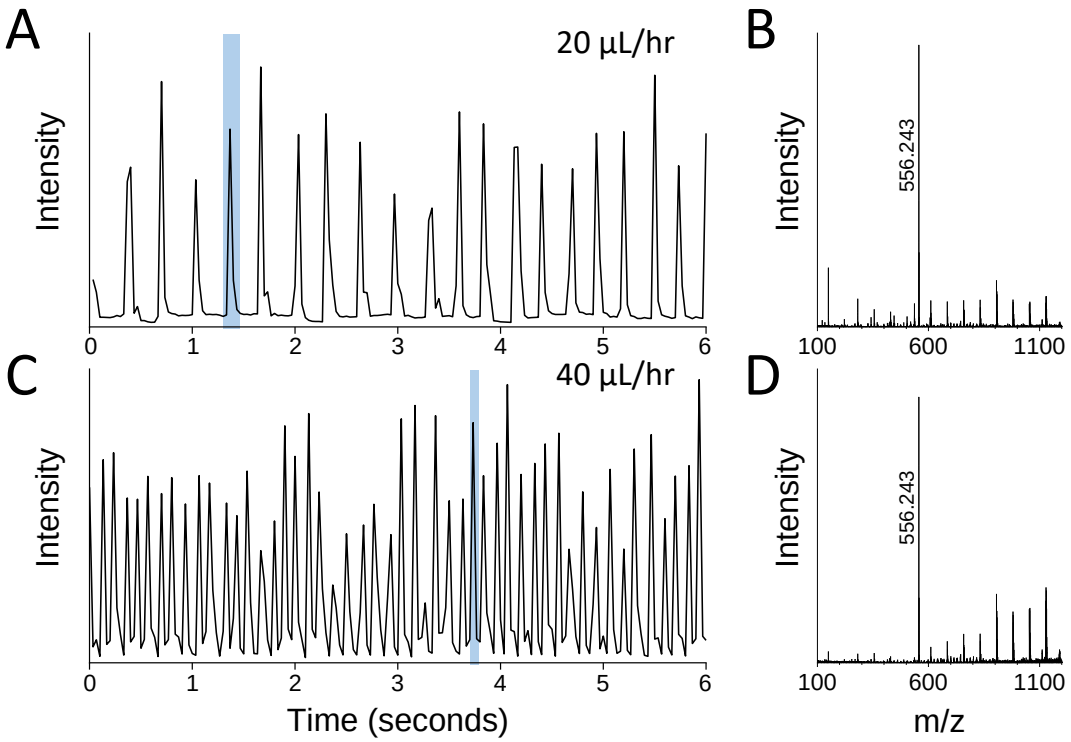

Figure 10: TIC and mass spectra obtained from the reinjection of LeuEnk droplets (~1 nL) into a Waters Synapt G2-Si mass spectrometer using the sprayer-chip interface with insulating base and grounding mesh connected. One peak in a chromatogram corresponds to one droplet detected by the mass spectrometer. The spacing oil flow rate was 200 µL/hr in both cases. A) Droplet infusion flow rate = 20 µL/hr resulting in a droplet reinjection rate equivalent to ~3.5 droplets/s. B) Mass spectrum obtained from one droplet peak in A (peak highlighted in blue). C) Droplet infusion flow rate = 40 µL/hr resulting in a droplet reinjection rate equivalent to ~8.5 droplets/s. D) Mass spectrum obtained from one droplet peak in C (peak highlighted in blue).

surfactant interaction, in combination with other field effects described by Zagnoni *et al*., results in the destabilisation of the oil film between two droplets in close proximity and thus, coalescence ensues.

Zagnoni *et al*. demonstrated that at voltages over a certain threshold, droplet coalescence upstream of the electrode region (rather than in direct electrical contact) was possible due to the penetration of the electric field. [58] In this work a larger voltage application (1000 V vs 20 V) has been applied to the droplet microfluidic system, and with this comes electric fields that permeate over an increased distance, such as the entire length of the microfluidic chip and into the

reinjection syringe. We hypothesize that a similar mechanism is occurring within the reinjection chip (design 1, Figure S1) and the higher voltages applied are penetrating the greater distance towards the reinjection spacing region in comparison to the shorter distances (and lesser voltages) demonstrated by Zagnoni.

To negate the coalescence effects described above, the most discernible solution is the act of distancing the adjoining droplet population from the electric field. This was achieved via lengthening the microfluidic chip (designs 3 and 4, Figure S1) and reversing the direction of the reinjection junction. This approach has been previously described by Peretzki *et al.* for the stable generation of droplets in glass microfluidic chips when coupling the chip outlet with an electrospray voltage. [43] The authors also consider an approach in which the entirety of the chip is 'floated' at the increased voltage required to generate an electrospray plume. [24] This would allow the droplets to avoid an electric field gradient when travelling towards the electrospray emitter, and hence retain a stable droplet flow. However, with droplet reinjection, care must be taken to also ensure the droplet reservoir and possibly syringe pumps also retain this increased electrical potential. This brings about several safety concerns regarding the placement of live voltages onto user accessible equipment and thus was not considered as a viable solution during this work. Peretzki *et al.* also note that the effect upon droplets under an applied electrical field is propagated to a greater extent in glass chips in comparison to those made of PDMS. [43] Thus, for MS coupled applications, any evolution of the microfluidic chip material in the future should be carefully considered.

Although distancing is a valid approach to reducing the electric field effects upon droplets, as the applied electrical voltage increases so does the field and the possibility that further distancing is required. As the chip design lengthens, its capacity to be described as 'miniaturised' decreases

and additionally the longer microfluidic channels serve increased back pressure upon the incoming droplets. Hence, there is a limit to such distancing approach and alternative solutions are sought. As shown in Figure 8 and 9, this was achieved by the insertion of an electrically conducting copper gauze, perpendicular to the channel plane as demonstrated by Schirmer *et al*. [39] This gauze was set to ground potential and successfully circumvented the electrical field generated by the electrospray voltage from penetrating the reinjection region upon application of 1 kV.

Due to the available HV probe utilised in the experiments performed under the microscope (Figure 8), the effects of voltages above 1 kV upon the chip with grounded gauze could not be confirmed. Initially, this was considered to be a barrier to the transferal of the apparatus to the MS, particularly as ESI often utilises voltages in the range of 1-5 kV. Upon closer inspection of the NanoLockSpray source HV cable, it was noted that the operator chosen voltage (e.g., 1-5 kV) was not the voltage applied directly to the sprayer block due to a 32 MΩ resistance incorporated into the HV cable (Waters part: 4185077BC1-S, resistor bands shown in Figure S11). For example, if +1 kV were applied by the operator software, +260 V would be placed upon the sprayer block and in proximity to the microfluidic chip. This provided a strong indication that the results obtained in Figure 8D (1000 V applied) would be suitable for transferal to the ESI push source platform up to a chosen ESI operator voltage of 3.8 kV (i.e., ~1000 V on the sprayer head).

As it had been determined that lower voltages were applied directly to the chip emitter than expected, it is possible that one of the two grounding solutions (i.e., distancing or grounding gauze) could be removed. Although this was not explored in these experiments, future iterations of the chip and source design may benefit from returning to shorter chip lengths or less connecting wires to ground. It is also important to note that as chip designs are altered to add greater functionalities, the coalescence negating effect of the grounding mesh may become less effective and thus should not be regarded as the sole solution to this challenge. The 3D printed sprayer

base is one alteration of the new source setup that should not be removed, particularly if it is to be replaced by a conductive material. Its insulating properties are critical to shielding the microfluidic chip from electric fields propagating from below the supporting glass slide.

Instrument Comparisons

The apparatus described in Figures 4 and 9, although fulfilling the droplet-reinjection-MS workflow, will require further development before becoming a user friendly and marketable solution for high throughput screening. For instance, the clamp stand utilised in the initial pull source setup (Figure 4) is not a permanent solution; the fluidic connections to the microfluidic chip are difficult to access. The Bruker pull source arrangement has gone some way to resolve this issue and replaced the clamp stand with a machined steel chip holder (Figure S5), which can be screwed directly onto the nebuliser block. This not only gives easier access to the fluidic inlets but also allows for smoother and more facile alteration of the emitter protrusion from the nebuliser outlet. In both pull source arrangements, this protrusion is not fixed and will require optimisation every time a new chip is interfaced. Thus, standardisation of the emitter distance from the end of the chip during chip fabrication would be a worthy undertaking.

Notably, both pull ESI sources from the two vendors apply a fixed position to the nebuliser block with respect to the MS inlet (i.e., no alteration in the X, Y or Z direction). Although this position will be the preferred location for single-phase electrospray, it must be considered whether this fixed position is optimal for droplet (i.e., dual-phase) electrospray. For example, the push source (Waters NanoLockSpray ESI) allows for such movement in the X, Y and Z directions, as well as alteration of the emitter protrusion. Alteration of these parameters may give rise to a position that is increasingly optimal for dual-phase electrospray. Conversely, fewer alterable parameters will increase the usability of the hardware setup, as trying to find the optimal position for the chip

outlet with respect to the MS inlet can become troublesome due to the vast number of possible positions. Upon comparing the two fixed pull source positions (Bruker v Agilent, Figure S4), it is clear that there is not only one possible location for the nebuliser to produce a stable electrospray plume. While Agilent's Dual-ESI source features a nebuliser directly perpendicular to the MS inlet, Bruker's ESI adopts a tilted position. It is possible that adopting alternative nebuliser positions results in an increase in ion transmission into the MS inlet and thus, a change in sensitivity between the two pull ESI sources. As sensitivity is also reliant on several other MS factors (for example Q-TOF v QIT) and droplet factors (e.g., size), several other experiments would be required to test this hypothesis and are beyond the scope of this article.

A major advantage to the push type source design in Figure 9 is the accessibility that manufacturers' stage provides to the chip. In this horizontal arrangement, the addition of the fluidic inlets is less cumbersome in comparison to the pull sources' upright or slanted arrangement (Figure S4). A secondary advantage to the stage is the possibility to add further fluidic structures beyond the current chip size, and still maintain a platform for the device to rest. Although this may be possible with the pull source, its upright nature is more fragile regards the emitter position and designing and building a scaffold around and above the source would be a more difficult task in comparison to using the currently available push source stage.

Considering the push source and its additional grounding solutions (Figure 9, Waters NanoLockSpray), the robustness of the setup requires improvement, and, in particular, the HV cable and 3D printed base attachments to the source stage and sprayer are fragile. Future iterations of the assembly should include several screw attachments within the 3D base design to more securely hold the sprayer head component as the original stainless-steel base does (Figure S8). In addition, an alteration of the base design to better contain the glass slide of the chip would be worthwhile to eliminate the use of reusable blue putty adhesive. The HV attachment to the

sprayer head could be more securely fixed via a small screw, as used in the original NanoLockSpray assembly, and would require alteration of the manufacturers' sprayer head design. This would be a welcomed addition from a safety perspective as the live HV cable is less likely to become loose during operation reducing the possibility of a shock to the operator.

Conclusions

To conclude, the integration of microfluidic chips with three vendors (nano)-ESI sources have been explored for droplet reinjection-MS workflows. Briefly, these sources have been segmented into those which apply the electrospray voltage directly to the incoming emitter (push type) and those which hold the emitter at ground potential (pull type). Pull type ESI sources fair well during the integration of the microfluidic chip, as only limited modifications to the manufacturer's source are required. The results obtained show clear rises and falls in the TIC corresponding to reinjected droplets. However, in the pull-type examples illustrated in this work, the need to position the chip vertical to the MS inlet may pose a problem for future additions to the apparatus due to inaccessibility around the chip location. Also, the requirement to incorporate an ESI needle of ~12 cm in length will result in increased back pressure within the chip channels. As the chip design evolves to include functionalities such as droplet splitting, this increase in backpressure could give rise to unwanted flow trajectory.

Push type ESI sources require the most modification to successfully couple droplet reinjection-microfluidic chips with MS. We have demonstrated that shielding or distancing of the reinjection region from the ESI voltage is of great importance; and in the case of the Waters SYNAPT G2-Si instrument, the setup also requires a modified base prepared from an insulating material. Implementing these modifications avoids coalescence of droplet populations prior to MS analysis, allowing for each droplet to be considered as a discrete reaction vessel. Furthermore, the chip

emitter interior must not be of conducting material for risk of droplet disruption. For example, the substitution of aluminium coated fused silica in place of the stainless-steel capillaries used previously. This being said, the greater accessibility of the stage employed by the push source exhibits greater potential to expand the chip functionalities beyond merely droplet reinjection.

In the immediate future, the development of these platforms will focus on apparatus robustness, in particular, the construction of a push source stage with components machined to more securely hold the microfluidic chip and sprayer head. Pull source modifications would benefit from the adaptation of the slide holder designed for the Bruker ESI source to more easily adjust the emitter protrusion distance out of the gas nebulising-port assembly. Applying this apparatus to a high throughput application within the biotechnology sector such as a directed evolution or biocatalysis workflow will also be key to raising the profile of this technology as a viable alternative to the traditional well plate methodologies. The current commercial ESI-Mine™ platform and associated microfluidic biochips have incorporated the functions of droplet splitting and MS signal-based sorting to address the destructive nature of MS on a pull type ion source mass spectrometer. The copper gauze shielding approach developed in this paper solved the droplet coalesces issue caused by an adjacent electrical field and allows the selection of ion source go beyond pull type only. This provides great flexibility to droplet microfluidics-MS technology, like ESI-Mine™, to be accommodated on a broader range of mass spectrometers with various ion sources from different vendors.

Author Contributions

EK performed the method development, chip fabrication and the majority of experimental procedures. CAS, XL and RS provided technical assistance and guidance. The 3D printed base was designed and fabricated by DS. Supervision was provided by AR and PEB. EK drafted and edited the manuscript with

input from all authors to the final form. A portion of this work was performed in collaboration with the EU ATTRACT Emerging Life (EmLife) project, in which EK contributed to the experimental work along with DM under the supervision of AMR. A supporting article detailing the outcomes from the EmLife project can be found at https://attract-eu.com/wp-content/uploads/2019/05/EmLife.pdf

Acknowledgements

Many thanks go to Dr Andy Currin and SYNBIOCHEM (The University of Manchester) for their cell culture assistance and training, and the use of their picodroplet encapsulation system. The authors would also like to thank the National Graphene Institute (The University of Manchester) for the use of their fabrication facilities and technical assistance. The use of gauze as a grounding solution would not have been possible without Dr Konstantin Wink, Dr Andrea Peretzki and Prof. Detlev Belder (University of Leipzig) sharing their expertise via E-mail, for which the authors are very grateful. We thank the FELIX Laboratory (Radboud University) for their kind hospitality, use of equipment and support with the projects, and Lisa Schultz for her assistance in the sample preparation of phenylalanine (F) and diphenylalanine (FF). EK, DM and AMR acknowledge the EU-ATTRACT project “Em-Life” for financial support. The authors would like to acknowledge Waters Corporation, and in particular Dr. Emrys Jones, for their support of our mass spectrometry development. We acknowledge the Engineering and Physical Sciences Research Council (EPSRC), the Biotechnology and Biological Sciences Research Council (BBSRC) and AstraZeneca plc for funding under the Prosperity Partnership EP/S005226/1, We acknowledge the support of EPSRC through the strategic equipment award EP/T019328/1, and BBSRC for funding the Centre for Synthetic Biology of Fine and Speciality Chemicals BB/M017702/1.

Conflicts of interest

Clive A. Smith and Xin Li are employed by Sphere Fluidics Limited which are a company that develops microfluidic devices that enables droplet delivery for cell screening applications. EK is now an employee of AstraZeneca, and owns stock or stock option, all experimental work and manuscript drafting was performed whilst in education at UoM.

Notes and references

1 G. Sun, L. Qu, F. Azi, Y. Liu, J. Li, X. Lv, G. Du, J. Chen, C.-H. Chen and L. Liu, *Biosens. Bioelectron.*, 2023, **225**, 115107.

2 R. Macarron, M. N. Banks, D. Bojanic, D. J. Burns, D. A. Cirovic, T. Garyantes, D. V. S. Green, R. P. Hertzberg, W. P. Janzen, J. W. Paslay, U. Schopfer and G. S. Sittampalam, *Nat. Rev. Drug Discov.*, 2011, **10**, 188–195.

3 J. P. Hughes, S. Rees, S. B. Kalindjian and K. L. Philpott, *Br. J. Pharmacol.*, 2011, **162**, 1239–1249.

4 S. A. Sundberg, *Curr. Opin. Biotechnol.*, 2000, **11**, 47–53.

5 A. A. Hajare, S. S. Salunkhe, S. S. Mali, S. S. Gorde, S. J. Nadaf and S. A. Pishawikar, *Am. J. Pharmtech Res.*, 2014, **4**, 112–129.

6 F. F. Bokhari and A. Albukhari, in *High-Throughput Screening for Drug Discovery*, ed. S. K. Saxena, IntechOpen, Rijeka, 2021, p. Ch. 4.

7 W. Zeng, L. Guo, S. Xu, J. Chen and J. Zhou, *Trends Biotechnol.*, 2020, **38**, 888–906.

8 B. Liu, S. Li and J. Hu, *Am. J. Pharmacogenomics*, 2004, **4**, 263–276.

9 H. K. Tamang, E. N. Stringham and B. E. Tourdot, *Curr. Protoc.*, 2023, **3**, e668.

10 O. H. Ajetunmobi, G. Wall, B. V Bonifacio, D. Montelongo-Jauregui and J. L. Lopez-Ribot, eds. D. J. Krysan and W. S. Moye-Rowley, Springer US, New York, NY, 2023, pp. 53–64.

11 C. Klopp, M. A. Struwe, C. Plieth, B. Clement and A. J. Scheidig, *Anal. Chem.*, 2023, **95**, 12452–

12458.

12 J. W. Armstrong, *Am. Biotechnol. Lab.*, 1999, **17**, 26–28.

13 P. Jacques, M. Béchet, M. Bigan, D. Caly, G. Chataigné, F. Coutte, C. Flahaut, E. Heuson, V. Leclère, D. Lecouturier, V. Phalip, R. Ravallec, P. Dhulster and R. Froidevaux, *Bioprocess Biosyst. Eng.*, 2017, **40**, 161–180.

14 S. Michael, D. Auld, C. Klumpp, A. Jadhav, W. Zheng, N. Thorne, C. P. Austin, J. Inglese and A. Simeonov, *Assay Drug Dev. Technol.*, 2008, **6**, 637–657.

15 L. Shang, Y. Cheng and Y. Zhao, *Chem. Rev.*, 2017, **117**, 7964–8040.

16 J. Panwar, A. Autour and C. A. Merten, *Nat. Protoc.*, 2023, **18**, 1090–1136.

17 L. Mazutis, J. Gilbert, W. L. Ung, D. A. Weitz, A. D. Griffiths and J. A. Heyman, *Nat. Protoc.*, 2013, **8**, 870–891.

18 J. J. Agresti, E. Antipov, A. R. Abate, K. Ahn, A. C. Rowat, J.-C. Baret, M. Marquez, A. M. Klibanov, A. D. Griffiths and D. A. Weitz, *Proc. Natl. Acad. Sci.*, 2010, **107**, 6550–6550.

19 Y.-C. Tan, J. S. Fisher, A. I. Lee, V. Cristini and A. P. Lee, *Lab Chip*, 2004, **4**, 292.

20 P. S. Dittrich and A. Manz, *Nat. Rev. Drug Discov.*, 2006, **5**, 210–218.

21 H. J. Butler, L. Ashton, B. Bird, G. Cinque, K. Curtis, J. Dorney, K. Esmonde-White, N. J. Fullwood, B. Gardner, P. L. Martin-Hirsch, M. J. Walsh, M. R. McAinsh, N. Stone and F. L. Martin, *Nat. Protoc.*, 2016, **11**, 664–687.

22 S. Mashaghi, A. Abbaspourrad, D. A. Weitz and A. M. van Oijen, *TrAC Trends Anal. Chem.*, 2016, **82**, 118–125.

23 Y. Zhu and Q. Fang, *Anal. Chim. Acta*, 2013, **787**, 24–35.

24 G. Perozziello, P. Candeloro, A. De Grazia, F. Esposito, M. Allione, M. L. Coluccio, R. Tallerico, I. Valpapuram, L. Tirinato, G. Das, A. Giugni, B. Torre, P. Veltri, U. Kruhne, G. Della Valle and E. Di

Fabrizio, *Opt. Express*, 2015, **24**, A180.

25 A. J. Oosthoek-De Vries, J. Bart, R. M. Tiggelaar, J. W. G. Janssen, P. J. M. Van Bentum, H. J. G. E. Gardeniers and A. P. M. Kentgens, *Anal. Chem.*, 2017, **89**, 2296–2303.

26 P. Hoffmann, U. Häusig, P. Schulze and D. Belder, *Angew. Chemie - Int. Ed.*, 2007, **46**, 4913–4916.

27 E. Fradet, C. Bayer, F. Hollfelder and C. N. Baroud, *Anal. Chem.*, 2015, **87**, 11915–11922.

28 S. Hassan, A. M. Nightingale and X. Niu, *Analyst*, 2016, **141**, 3266–3273.

29 M. P. Cecchini, J. Hong, C. Lim, J. Choo, T. Albrecht, A. J. deMello and J. B. Edel, *Anal. Chem.*, 2011, **83**, 3076–3081.

30 A. M. Kaushik, K. Hsieh, L. Chen, D. J. Shin, J. C. Liao and T. H. Wang, *Biosens. Bioelectron.*, 2017, **97**, 260–266.

31 T. Beneyton, S. Thomas, A. D. Griffiths, J.-M. Nicaud, A. Drevelle and T. Rossignol, *Microb. Cell Fact.*, 2017, **16**, 18.

32 T. Beneyton, I. P. M. Wijaya, P. Postros, M. Najah, P. Leblond, A. Couvent, E. Mayot, A. D. Griffiths and A. Drevelle, *Sci. Rep.*, 2016, **6**, 27223.

33 B. E. Murray, L. I. Penabad and R. T. Kennedy, *Curr. Opin. Biotechnol.*, 2023, **82**, 102962.

34 V. Plekhova, K. De Windt, M. De Spiegeleer, M. De Graeve and L. Vanhaecke, *TrAC Trends Anal. Chem.*, 2023, **168**, 117287.

35 G. R. D. Prabhu, E. R. Williams, M. Wilm and P. L. Urban, *Nat. Rev. Methods Prim.*, 2023, **3**, 23.

36 C. A. Smith, X. Li, T. H. Mize, T. D. Sharpe, E. I. Graziani, C. Abell and W. T. S. Huck, *Anal. Chem.*, 2013, **85**, 3812–3816.

37 K. Wink, L. Mahler, J. R. Beulig, S. K. Piendl, M. Roth and D. Belder, *Anal. Bioanal. Chem.*, 2018, **410**, 7679–7687.

38 X. W. Diefenbach, I. Farasat, E. D. Guetschow, C. J. Welch, R. T. Kennedy, S. Sun and J. C. Moore, *ACS Omega*, 2018, **3**, 1498–1508.

39 M. Schirmer, K. Wink, S. Ohla, D. Belder, A. Schmid and C. Dusny, *Anal. Chem.*, 2020, **92**, 10700–10708.

40 L. Mahler, K. Wink, R. J. Beulig, K. Scherlach, M. Tovar, E. Zang, K. Martin, C. Hertweck, D. Belder and M. Roth, *Sci. Rep.*, 2018, **8**, 13087.

41 ESI-Mine™: A label-free platform for high-throughput, miniaturised electrospray injection mass spectrometry (ESI-MS).

42 X. C. I. Solvas and A. deMello, *Chem. Commun.*, 2011, **47**, 1936–1942.

43 A. J. Peretzki, S. Schmidt, E. Flachowsky, A. Das, R. F. Gerhardt and D. Belder, *Lab Chip*, 2020, **20**, 4456–4465.

44 K. Choi, A. H. C. Ng, R. Fobel and A. R. Wheeler, *Annu. Rev. Anal. Chem.*, 2012, **5**, 413–440.

45 J. C. Mcdonald, D. C. Duffy, J. R. Anderson and D. T. Chiu, *Electrophoresis*, 2000, **21**, 27–40.

46 S. Tang and G. Whitesides, in *Optofluidics: Fundamentals, Devices, and Applications*, 2010, pp. 7–32.

47 E. E. Kempa, C. A. Smith, X. Li, B. Bellina, K. Richardson, S. Pringle, J. L. Galman, N. J. Turner and P. E. Barran, *Anal. Chem.*, 2020, **92**, 12605–12612.

48 D. Morsa, E. Kempa, I. Stroganova, A. Piruska, W. T. S. Huck, P. Nghe, E. Szathmáry, W. Hordijk, J. Commandeur, S. Otto and A. M. Rijs, in *Public deliverable for the ATTRACT Final Conference*, 2020.

49 D. Sarkar, E. Sinclair, S. H. Lim, C. Walton-Doyle, K. Jafri, J. Milne, J. P. C. Vissers, K. Richardson, D. K. Trivedi, M. Silverdale and P. Barran, *JACS Au*, 2022, **2**, 2013–2022.

50 N. Bremond, A. R. Thiam and J. Bibette, *Phys. Rev. Lett.*, 2008, **100**, 1–4.

51 X. Niu, S. Gulati, J. B. Edel and A. J. deMello, *Lab Chip*, 2008, **8**, 1837.

52 C. N. Baroud, M. Robert De Saint Vincent and J. P. Delville, *Lab Chip*, 2007, **7**, 1029–1033.

53 M. Zagnoni, G. Le Lain and J. M. Cooper, *Langmuir*, 2010, **26**, 14443–14449.

54 A. Srivastava, S. Karthick, K. S. Jayaprakash and A. K. Sen, *Langmuir*, 2018, **34**, 1520–1527.

55 S. K. Cho, H. Moon and C. J. Kim, *J. Microelectromechanical Syst.*, 2003, **12**, 70–80.

56 M. G. Pollack, A. D. Shenderov and R. B. Fair, *Lab Chip*, 2002, **2**, 96–101.

57 J. C. Baret, O. J. Miller, V. Taly, M. Ryckelynck, A. El-Harrak, L. Frenz, C. Rick, M. L. Samuels, J. B. Hutchison, J. J. Agresti, D. R. Link, D. A. Weitz and A. D. Griffiths, *Lab Chip*, 2009, **9**, 1850–1858.

58 M. Zagnoni, C. N. Baroud and J. M. Cooper, *Phys. Rev. E - Stat. Nonlinear, Soft Matter Phys.*, 2009, **80**, 046303.

59 G. Etienne, M. Kessler and E. Amstad, *Macromol. Chem. Phys.*, 2017, **218**, 1600365.